



**HAL**  
open science

# Cryogenic Chemistry and Quantitative Non-Thermal Desorption from Pure Methanol Ices: High-Energy Electron versus X-Ray Induced Processes

Daniela Torres-Díaz, Romain Basalgète, Mathieu Bertin, Jean-Hugues Fillion, Xavier Michaut, Lionel Amiaud, Anne Lafosse

► **To cite this version:**

Daniela Torres-Díaz, Romain Basalgète, Mathieu Bertin, Jean-Hugues Fillion, Xavier Michaut, et al.. Cryogenic Chemistry and Quantitative Non-Thermal Desorption from Pure Methanol Ices: High-Energy Electron versus X-Ray Induced Processes. *ChemPhysChem*, 2023, 10.1002/cphc.202200912 . hal-03971378

**HAL Id: hal-03971378**

**<https://hal.science/hal-03971378v1>**

Submitted on 3 Feb 2023

**HAL** is a multi-disciplinary open access archive for the deposit and dissemination of scientific research documents, whether they are published or not. The documents may come from teaching and research institutions in France or abroad, or from public or private research centers.

L'archive ouverte pluridisciplinaire **HAL**, est destinée au dépôt et à la diffusion de documents scientifiques de niveau recherche, publiés ou non, émanant des établissements d'enseignement et de recherche français ou étrangers, des laboratoires publics ou privés.



Distributed under a Creative Commons Attribution 4.0 International License

## Accepted Article

**Title:** Cryogenic Chemistry and Quantitative Non-Thermal Desorption from Pure Methanol Ices: High-Energy Electron versus X-Ray Induced Processes

**Authors:** Daniela Torres-Díaz, Romain Basalgète, Mathieu Bertin, Jean-Hugues Fillion, Xavier Michaut, Lionel Amiaud, and Anne LAFOSSE

This manuscript has been accepted after peer review and appears as an Accepted Article online prior to editing, proofing, and formal publication of the final Version of Record (VoR). The VoR will be published online in Early View as soon as possible and may be different to this Accepted Article as a result of editing. Readers should obtain the VoR from the journal website shown below when it is published to ensure accuracy of information. The authors are responsible for the content of this Accepted Article.

**To be cited as:** *ChemPhysChem* **2023**, e202200912

**Link to VoR:** <https://doi.org/10.1002/cphc.202200912>

## RESEARCH ARTICLE

# Cryogenic Chemistry and Quantitative Non-Thermal Desorption from Pure Methanol Ices: High-Energy Electron versus X-Ray Induced Processes

Daniela Torres-Díaz,<sup>[a,b]</sup> Romain Basalgète,<sup>[b]</sup> Mathieu Bertin,<sup>[b]</sup> Jean-Hugues Fillion,<sup>[b]</sup> Xavier Michaut,<sup>[b]</sup> Lionel Amiaud,<sup>[a]</sup> and Anne Lafosse\*<sup>[a]</sup>

[a] D. Torres-Díaz, Asc. Prof. L. Amiaud, Prof. A. Lafosse  
Université Paris-Saclay, CNRS, Institut des Sciences Moléculaires d'Orsay  
91405 Orsay, France  
E-mail: anne.lafosse@universite-paris-saclay.fr

[b] D. Torres-Díaz, R. Basalgète, Asc. Prof. M. Bertin, Prof. J.-H. Prof. Fillion, X. Michaut  
Laboratoire d'Etudes du Rayonnement et de la Matière en Astrophysique et Atmosphères (LERMA)  
Sorbonne Université, Observatoire de Paris, PSL University, CNRS  
4 Pl. Jussieu, 75005 Paris, France

Supporting information for this article is given via a link at the end of the document.

**Abstract:** X-Ray irradiation of interstellar ice analogues has recently been proven to induce desorption of molecules, thus being a potential source for the still-unexplained presence of gaseous organics in the coldest regions of the interstellar medium, especially in protoplanetary disks. The proposed desorption mechanism involves the Auger decay of excited molecules following soft X-ray absorption, known as X-ray induced electron-stimulated desorption (XESD). Aiming to quantify electron induced desorption in XESD, we irradiated pure methanol (CH<sub>3</sub>OH) ices at 23 K with 505 eV electrons, to simulate the Auger electrons originating from the O 1s core absorption. Desorption yields of neutral fragments and the effective methanol depletion cross-section were quantitatively determined by mass spectrometry. We derived desorption yields in molecules per incident electron for CO, CO<sub>2</sub>, CH<sub>3</sub>OH, CH<sub>4</sub>/O, H<sub>2</sub>O, H<sub>2</sub>CO, C<sub>2</sub>H<sub>6</sub> and other less abundant, but more complex organic products. We obtained desorption yields remarkably similar to XESD values.

## Introduction

Methanol (CH<sub>3</sub>OH) is an important molecule detected in the interstellar medium (ISM) and is considered a precursor for larger and more complex molecules in both gas and solid phases.<sup>[1]</sup> Its abundance in ice mantles covering interstellar dust grains is estimated to be between 1% and 25% relative to water, the highest after CO<sub>2</sub> and CO,<sup>[2]</sup> and it is usually thought to form via successive hydrogenations of carbon monoxide in the ice.<sup>[3,4]</sup> In low temperature environments (10-30 K), where thermal desorption from the ice mantle is negligible, non-thermal desorption processes are necessary to explain the observed gas phase methanol abundance. Non-thermal desorption mechanisms include sputtering by cosmic rays,<sup>[5]</sup> photodesorption,<sup>[6-9]</sup> and desorption due to the exothermicity of surface reactions.<sup>[10]</sup> Each of these processes needs to be both quantified and understood at a molecular scale in order to be incorporated in astrochemical models, and ultimately in order to estimate their respective role in the observed gas phase abundances of methanol in star and planet-forming regions.

Regarding photodesorption, for pure methanol and mixed ices with CO, studies have focused mainly on the desorption induced by vacuum UV photons, at the hydrogen Lyman-alpha or in the whole 7 to 14 eV energy range.<sup>[6,9]</sup> More recently, X-rays have gained attention as a photon source relevant in regions such as protoplanetary disks, where young stellar objects emit X-rays in the range 0.1-10 keV.<sup>[8,11a,11b,12]</sup> In particular, X-ray induced electron-stimulated desorption (XESD) has been suggested to be the dominant mechanism explaining the observed desorption of neutral species in irradiation of interstellar ice analogues with 500-600 eV X-rays.<sup>[8,11a,11b]</sup> It has been proposed that this mechanism is driven by the thermalization of Auger electrons generated in the solid by the decay of core excited or ionized molecules, although no direct evidence has been provided.

The KLL Auger electrons originating from an O 1s core absorption (~505 eV for condensed methanol,<sup>[13]</sup> 99.4% yield<sup>[14]</sup>) generate a large amount of low energy secondary electrons (LEE, <25 eV) and excitons in the ice. For instance, in the case of water ice, one 500 eV electron is expected to create around 25 secondary ones.<sup>[15]</sup> These LEE can induce different processes depending on their energy, such as dissociative electron attachment (DEA), neutral dissociation (ND), dipolar dissociation (DD), dissociative ionization (DI), and desorption induced by electronic transitions (DIET) of neutral species.<sup>[16-19]</sup> The reactive species generated in the ice via the dissociative pathways can also lead to electron induced synthesis, contributing to the chemical complexity of the ice.<sup>[19]</sup>

Several studies of electron irradiation of methanol, at both low and high energies, have focused on the chemical evolution of the irradiated ice and on the enrichment of the gas phase. In these studies, mechanisms explaining product formation were also discussed.<sup>[20-26]</sup> But to our knowledge, no quantitative values have been provided for neutral desorption during electron irradiation. Accordingly, direct comparisons between the desorption efficiencies driven by X-rays at the O K-edge and primary electrons whose energy mimics the Auger electron photogenerated in the ice are missing.

## RESEARCH ARTICLE

Here we present quantitative desorption yields for methanol and several products, in molecules per incident electron, for pure methanol ices irradiated with 505 eV electrons. The observed efficient chemical modification of the ice will be described quantitatively in terms of an effective methanol depletion cross-section, and this parameter interpreted to obtain the desorption relevant depth, i.e. the ice thickness involved in the desorption processes. The irradiation experiments allowed us to evaluate the contribution of Auger electrons generated in the ice upon X-Ray absorption. By comparing the yields measured under X-ray irradiation,<sup>[8]</sup> the dominant role played by XESD and the thermalization of the generated Auger electron is clearly demonstrated.

Methanol ices, typically 70 to 100 monolayers (ML) thick, were grown by vapour deposition on a cold substrate (23 K) and irradiated with 505 eV electrons. The Electron Stimulated Desorption (ESD) of neutral molecules during irradiation was monitored with a Quadrupole Mass Spectrometer (QMS) equipped with an electron ionization source. Up to ten m/z fragments were recorded during irradiation, as a function of electron flux, accumulated electron dose and ice thickness. Temperature Programmed Desorption (TPD) was used to calibrate the QMS signal and to probe the post-irradiation ice residues. First, we will discuss the quantitative data obtained for methanol from the ESD experiments, followed by the induced chemistry and finally a comparison between electron and X-Ray induced absolute desorption yields.

## Results and Discussion

### Methanol Desorption Yield

To quantify methanol desorption during irradiation with 505 eV electrons we used the fragment m/z 32, corresponding to the molecular ion CH<sub>3</sub>OH<sup>+</sup> formed at the QMS head. An example of the desorption signal, which decays exponentially with increasing fluence (accumulated electron dose), is shown in Figure 1a. Similar behaviour was observed in all experiments at different electron fluxes and ice thicknesses. For the early irradiation stage, a first-order kinetics fit was done to extract two quantitative parameters: the initial desorption yield Y<sub>0</sub> and the effective cross-section σ<sub>eff</sub>.

The errors for Y<sub>0</sub> and σ<sub>eff</sub> given throughout the paper result from the statistical uncertainties of this fit (typically 5% for Y<sub>0</sub> and 10 % σ<sub>eff</sub>) but it should also be noticed that the uncertainties in electron flux read (±20%) and beam size (±8%) give an estimated systematic error of 13% for Y<sub>0</sub> and 9% for σ<sub>eff</sub>. The values for methanol's initial desorption yield Y<sub>0</sub> (in counts per electron, cts/e<sup>-</sup> for short) are converted into absolute yields Γ<sub>0</sub> (in molecules/e<sup>-</sup>) following the method described in the experimental section and detailed in the Supporting Information. The uncertainty related to this method used to calculate Γ<sub>0</sub> is estimated to be 50%. Results from systematic experiments are summarised in Figure 1b. It is shown for a broad range of fluxes and thicknesses that Γ<sub>0</sub>(CH<sub>3</sub>OH) is in the range of 0.12 to 0.26 molecules/e<sup>-</sup>. The weighted-average value for all the experiments is taken, which

corresponds to 0.15±0.01 molecules/e<sup>-</sup>. We interpret this as the desorption induced by the very first electrons impinging on the pristine methanol ice, which agrees with the observation that values are independent of irradiation flux. Y<sub>0</sub> and Γ<sub>0</sub> show no correlation to film thickness in the range of thicknesses used, excluding substrate contributions and confirming that we work in a semi-infinite thickness regime.

### Effective Depletion Cross-Section

The fact that the methanol desorption signal (Figure 1a) shows a non-zero order decay is attributed to the modification of the original methanol ice via electron-induced chemical reactions. If intact methanol molecule desorption were the only ice depletion mechanism, we would expect the yield to depend only on the amount of methanol molecules available at the surface.<sup>[7]</sup> Therefore, the yield would not change with irradiation fluence in the semi-infinite regime, i.e. for ice multilayers thick enough to prevent substrate and thickness effects. The parameter σ<sub>eff</sub>, referred to as "effective cross-section", characterises the efficiency of the chemical modification taking place. It is related to all processes leading to methanol depletion in the probed ice depth, i.e. fragmentation, chemical reactions and desorption. The σ<sub>eff</sub> determined from m/z 32, at different electron fluxes and ice thicknesses, ranges between 5×10<sup>-16</sup> and 15×10<sup>-16</sup> cm<sup>2</sup> (Fig. S3). The weighted-average value is (7.7±0.3)×10<sup>-16</sup> cm<sup>2</sup>. This is of the same order of magnitude as the water EPD (Electron-Promoted Desorption) cross-section from compact amorphous solid water upon irradiation with 200-300 eV electrons, which was found to increase in said energy range from 1.6×10<sup>-16</sup> to 5.2×10<sup>-16</sup> cm<sup>2</sup>.<sup>[27]</sup> Dupuy *et al.*<sup>[116]</sup> performed ESD experiments on molecular ices as a function of electron energy (150-2000 eV) and introduced the concept of *desorption relevant depth*. The authors related it to the dominant energy and/or particle transport mechanism(s) leading to desorption, including chemical modification processes. The depletion cross-section σ<sub>eff</sub> can be converted into a characteristic depth involved in methanol desorption upon electron irradiation at 505 eV, according to equation (1):<sup>[28]</sup>

$$\Lambda_c = 1/(\sigma_{\text{eff}}N) \quad (1)$$

Where N is the molecular density of the ice. Using a density of 0.64 g/cm<sup>3</sup><sup>[29]</sup> we obtain N = 1.20 × 10<sup>22</sup> molecules/cm<sup>3</sup> and Λ<sub>c</sub> = 11.2 Å, i.e. 2.6 monolayers (ML). Assuming an exponential attenuation (equation (2)) of the electron-induced processes that lead to desorption:

$$I_t = I_0 \exp -(d/\Lambda_c) \quad (2)$$

We consider that a total depth (d) of Λ<sub>des</sub> = 3 × Λ<sub>c</sub> ≈ 8 ML contributes to the observed desorption. At the same time, said depth undergoes chemical modification, but this does not rule out that chemical processing can occur deeper in the ice as well. The calculated Λ<sub>des</sub> is comparable to the penetration depth of the incoming 505 eV electrons estimated from the electron Inelastic Mean Free Path (IMFP) in organic materials (11 ML)<sup>[30,31]</sup> and to Monte Carlo simulations (14 ML).<sup>[32]</sup>

## RESEARCH ARTICLE

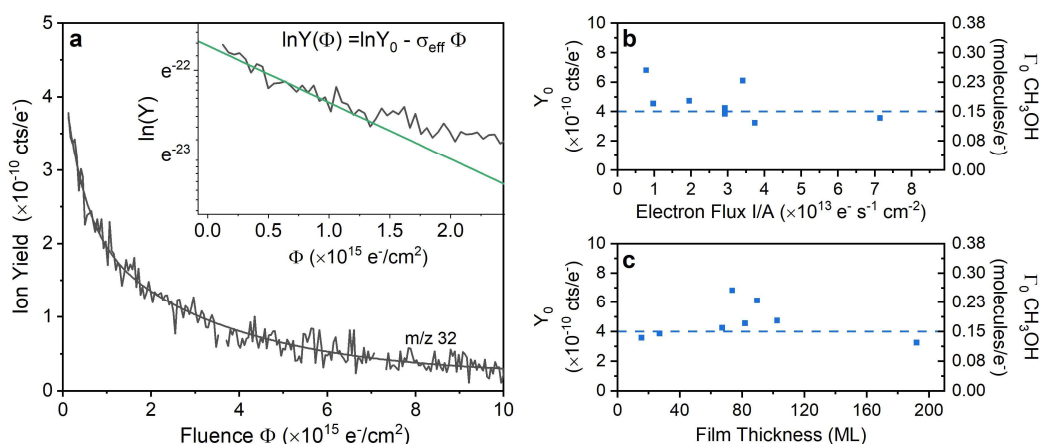


**Figure 1.** a) ESD profile of  $m/z$  32 recorded during 505 eV electron irradiation (flux  $2.9 \times 10^{13} \text{ s}^{-1} \text{ cm}^{-2}$ ) of a pure methanol ice (70 ML) at 23K. Inset shows the linear fit of the early irradiation stage signal, which gives the parameters  $Y_0$  and  $\sigma_{\text{eff}}$ . b) Desorption yields  $Y_0$  for  $m/z$  32 (cts/e $^-$ ) and corresponding  $\Gamma_0$   $\text{CH}_3\text{OH}$  (molecules/e $^-$ ) versus electron flux and c) versus methanol ice thickness. Dashed line corresponds to the weighted-average value, calculated by taking into account the statistical uncertainty of the fits:  $(4.0 \pm 0.3) \times 10^{-10}$  cts/e $^-$  for  $Y_0$  and  $0.15 \pm 0.01$  molecules/e $^-$  for  $\Gamma_0(\text{CH}_3\text{OH})$ .

### Electron Induced Chemistry

As mentioned above, there is clear evidence of efficient chemical modification of the methanol ice, probed via its non-thermal desorption signature. These processes contribute to the enrichment of the chemical species present in the gas phase in the ISM.

Several desorption signals are too high to be ascribed to methanol cracking at the QMS: 10% of the total  $m/z$  31  $Y_0$  is attributed either to desorbing  $\text{CH}_3\text{O}/\text{CH}_2\text{OH}$  radical fragments or to the cracking of products of higher molecular mass, while 80% of the total  $m/z$  30  $Y_0$ , 98% of the total  $m/z$  28 and 60% of the total  $m/z$  29  $Y_0$  must have other origins. Similarly, methanol can only account for a minimal part of the observed  $m/z$  16 and 18. Finally, fragments not related to methanol cracking at the QMS ( $m/z$  26, 27, 44, 46, 60 and 61) are clearly detected desorbing during irradiation. This is due to desorption of new neutral molecules or fragments synthesized within the ice. As observed for  $m/z$  32, there is no correlation between  $Y_0$  and electron flux for any recorded fragment (Figure S4).

Several compounds contribute to the observed  $m/z$ , therefore products of methanol irradiation mentioned in literature were considered as a starting point for attribution: CO (carbon monoxide),  $\text{CO}_2$  (carbon dioxide),  $\text{CH}_4$  (methane),  $\text{H}_2\text{O}$  (water),  $\text{H}_2\text{CO}$  (formaldehyde),  $\text{C}_2\text{H}_6$  (ethane),  $\text{CH}_3\text{OCH}_3$  (dimethyl ether, DME) and  $\text{CH}_3\text{CH}_2\text{OH}$  (ethanol, EtOH),  $\text{HCOOH}$  (formic acid, FA),  $\text{OHCH}_2\text{CH}_2\text{OH}$  (ethylene glycol, EG),  $\text{HCOOCH}_3$  (methyl formate, MF),  $\text{CH}_3\text{COOH}$  (acetic acid, AcOH),  $\text{OHCH}_2\text{CHO}$  (glycolaldehyde, GA),  $\text{CH}_3\text{OCH}_2\text{OH}$  (methoxymethanol, MM) and  $\text{HOCH}_2\text{CH}(\text{OH})\text{CH}_2\text{OH}$  (glycerine or glycerol, GC).

The main molecules seen desorbing were CO,  $\text{CO}_2$ ,  $\text{CH}_4$ ,  $\text{H}_2\text{O}$  and  $\text{H}_2\text{CO}$ , all previously identified in ESD experiments with 100 eV electrons by Akin *et al.*,<sup>[22]</sup> and with low energy electrons (<20 eV) by Schmidt *et al.*<sup>[21]</sup> They have also been detected in-situ in the processed ice by infrared spectroscopy (IR) during 5 keV electron irradiation by Maity *et al.*,<sup>[23]</sup> 10 keV electron irradiation by Mahjoub *et al.*,<sup>[25]</sup> and UV photon irradiation by Öberg *et al.*<sup>[7]</sup> To the best of our knowledge,  $\text{C}_2\text{H}_6$  (ethane) has only been identified as an irradiation product in ESD experiments of pure methanol ices with 100 eV electrons by Akin *et al.*,<sup>[22]</sup> although it

was also identified by Öberg *et al.*<sup>[7]</sup> in an irradiated  $\text{CH}_3\text{OH}:\text{CH}_4$  ice, and it is an expected product of  $\text{CH}_3$  radical recombination.<sup>[21,26]</sup> Products such as  $\text{CH}_3\text{OCH}_3$  (DME) and  $\text{CH}_3\text{CH}_2\text{OH}$  (EtOH) have been identified in several of the above mentioned studies<sup>[7,21,23]</sup> and in post-irradiation TPD by Harris *et al.*<sup>[20]</sup> (55 eV electrons) and Boamah *et al.*<sup>[26]</sup>  $\text{HCOOH}$  (FA) was detected in-situ by IR spectroscopy after photon irradiation with soft X-rays by Chen *et al.*<sup>[33]</sup> and after UV irradiation by Öberg *et al.*<sup>[7]</sup> Heavier products (molecular mass  $\geq 60$  a.u) have also been identified in the ice residues after irradiation with electrons or photons, for several irradiation energies. Yet, they have never been observed desorbing during irradiation. For instance ethylene glycol,<sup>[7,20,21,23–26,33,34]</sup> as well as methyl formate,<sup>[7,23,26,33,34]</sup> acetic acid,<sup>[7,26,33]</sup> glycolaldehyde,<sup>[23,26,33,34]</sup> methoxymethanol,<sup>[20,21,23,26,35]</sup> and glycerine or glycerol.<sup>[24,26]</sup>

The mass fragmentation patterns available in the NIST database<sup>[36]</sup> were used to analyse our results. The histogram shown in Figure 2 was constructed with the average  $Y_0$  values for each  $m/z$  (a summary table is also available Table S1).

The early stage desorption yields  $Y_0$  (cts/e $^-$ ) were converted, after attributions, into desorbed molecules per incident electron ( $\Gamma_0$ ) according to the electron ionisation cross-sections available in the literature. For the cases where unequivocal attributions cannot be done (i.e. similar mass fragmentation patterns), we can only provide an order of magnitude.

A set of experiments was dedicated to obtaining the yields of  $m/z$  16, 18, 28 and 44. These masses are confidently attributed mostly to, respectively:  $\text{CH}_4/\text{O}$ ,  $10^{-1}$  mol./e $^-$ ;  $\text{H}_2\text{O}$ ,  $(7.4 \pm 0.1) \times 10^{-2}$  mol./e $^-$ ; CO,  $1.1 \pm 0.1$  mol./e $^-$  and  $\text{CO}_2$ ,  $(2.5 \pm 0.2) \times 10^{-1}$  mol./e $^-$ . These yields remain estimates since the residual gas in the vacuum chamber is known to affect said mass channels.

Fragment  $m/z$  26 can originate from  $\text{C}_2\text{H}_6$  (ethane) and ethanol. For the latter, according to its fragmentation pattern, the intensity of  $m/z$  26 is about 45% that of  $m/z$  46. Since the total  $m/z$  46 signal is about 5 times smaller than the  $m/z$  26, we estimate that at least 92% of the  $m/z$  26 signal is due to  $\text{C}_2\text{H}_6$ , corresponding to a  $\Gamma_0$  of  $(3.2 \pm 0.3) \times 10^{-2}$  molecules per electron. The average value for  $m/z$  27 is comparable to the one for  $m/z$  26 (see Fig. S4), which agrees well with  $\text{C}_2\text{H}_6$  being the main contributor to these two fragments.

## RESEARCH ARTICLE

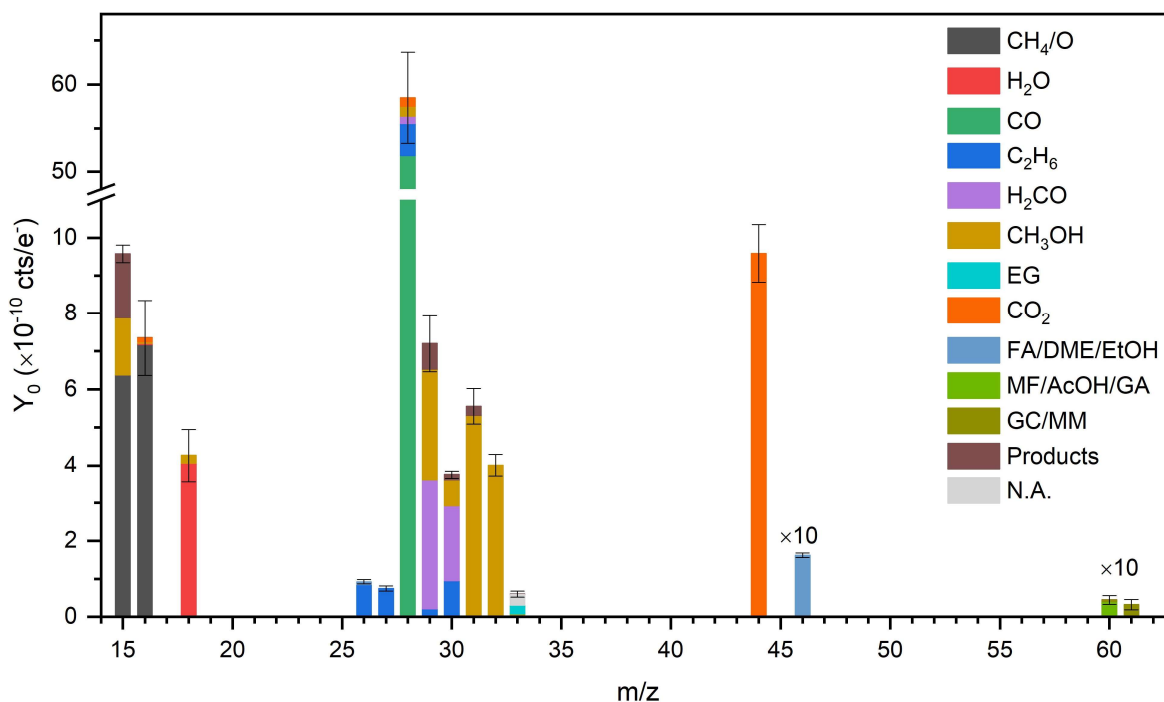


**Figure 2.** ESD yields ( $Y_0$ ) measured for different  $m/z$  fragments at the early irradiation stage. Different molecules contribute to the fragments as shown with the colour code. See text for detail on attribution criteria. EG: ethylene glycol, FA: formic acid, DME: dimethyl ether, EtOH: ethanol, MF: methyl formate, AcOH: acetic acid, GA: glycolaldehyde, GC: glycerine, MM: methoxymethanol, Products: corresponding radicals desorbing as neutrals and/or QMS fragments from heavier products, N.A.: non-attributed.

Interestingly, the ratio between fragments  $m/z$  31 and 30 does not vary much for the different products considered here, with  $m/z$  30 corresponding to 7% to 20% of the  $m/z$  31 signal (Figure 2, brown), except for  $H_2CO$  and  $C_2H_6$ , which do not produce the  $m/z$  31 fragment. The remaining  $m/z$  30 signal, after taking into account  $CH_3OH$  and  $C_2H_6$  contributions to this mass channel, is therefore attributed to formaldehyde ( $H_2CO$ ) desorption and corresponds to  $(3.6 \pm 0.4) \times 10^{-2}$  molecules per electron.

Regarding the heavier fragment  $m/z$  46, it can correspond to dimethyl ether, ethanol and formic acid, which have similar fragmentation patterns. We estimate a total yield of  $10^{-3}$  to  $10^{-2}$  molecules per electron. Fragment  $m/z$  61, could originate from glycerine and methoxymethanol, corresponding to a yield of  $10^{-3}$  molecules per electron. These two molecules are minor contributors to the observed  $m/z$  60 and 33 during ESD. At least 91% of the  $m/z$  60 signal could come from methyl formate, acetic acid and glycolaldehyde, with a total yield of  $10^{-3}$  molecules per electron.

The fragment  $m/z$  46 was also detected in the gas phase upon soft X-ray irradiation of pure methanol ices,<sup>[8]</sup> but for fragments  $m/z$  60 and 61 this is a first report of desorption during irradiation. Even though the yields for these fragments are much lower compared to others, the desorption signals were clearly detected. The presence of a molecule in TPD experiments is further proof supporting the identification of synthesised products seen during ESD. Qualitative analysis of post-irradiation residues using TPD gives information about molecules remaining in the ice after irradiation, according to their different desorption temperatures. Since the environment of the molecules affects said temperatures,

we rely on available literature data for similar ices to analyse our results (see references cited earlier for each molecule). The TPD curves for  $m/z$  61 and 62 (Supporting Information, Figure S5) show characteristic desorption peaks for methoxymethanol ( $CH_3OCH_2OH$ ) and ethylene glycol ( $OHCH_2CH_2OH$ ), respectively, supporting our interpretation of the desorption signals. We also observed  $m/z$  46 desorption peaks consistent with dimethyl ether ( $CH_3OCH_3$ ) and ethanol ( $CH_3CH_2OH$ ) (not shown).

The last interesting fragment detected desorbing during irradiation was  $m/z$  33. Contribution from methoxymethanol is negligible, while for ethylene glycol the associated  $m/z$  31 signal should be almost three times higher than  $m/z$  33, yet both values are comparable (Fig. S4). This leads to the conclusion that at most 45% of the observed  $m/z$  33 yield could be due to ethylene glycol, this being likely an overestimation.

The formation of another molecule which contributes to  $m/z$  33 but not  $m/z$  31, such as  $H_2O_2$  or  $HO_2$ , would explain what we observe. It is known that UV irradiation of condensed methanol at 157 nm (7.9 eV) leads to OH formation,<sup>[37]</sup> so this radical is reasonably expected in our electron irradiation experiments too. Radical chemistry in water ices involving OH yields  $H_2O_2$  and  $HO_2$ , which in turn are precursors of  $O_2$ .<sup>[38]</sup> However, hydrogen peroxide ( $H_2O_2$ ) can be excluded here since we did not observe  $m/z$  34 desorbing during electron irradiation of methanol. The non-assigned yield of  $m/z$  33 in our experiments (Figure 2, light grey) could then correspond to  $HO_2$  desorbing.

All the yields in molecules per incident electron ( $\Gamma_0$ ) are summarised in Figure 3. The main products seen desorbing, in decreasing order, were CO,  $CO_2$ ,  $CH_4/O$ ,  $H_2O$ ,  $H_2CO$  and  $C_2H_6$ .

## RESEARCH ARTICLE

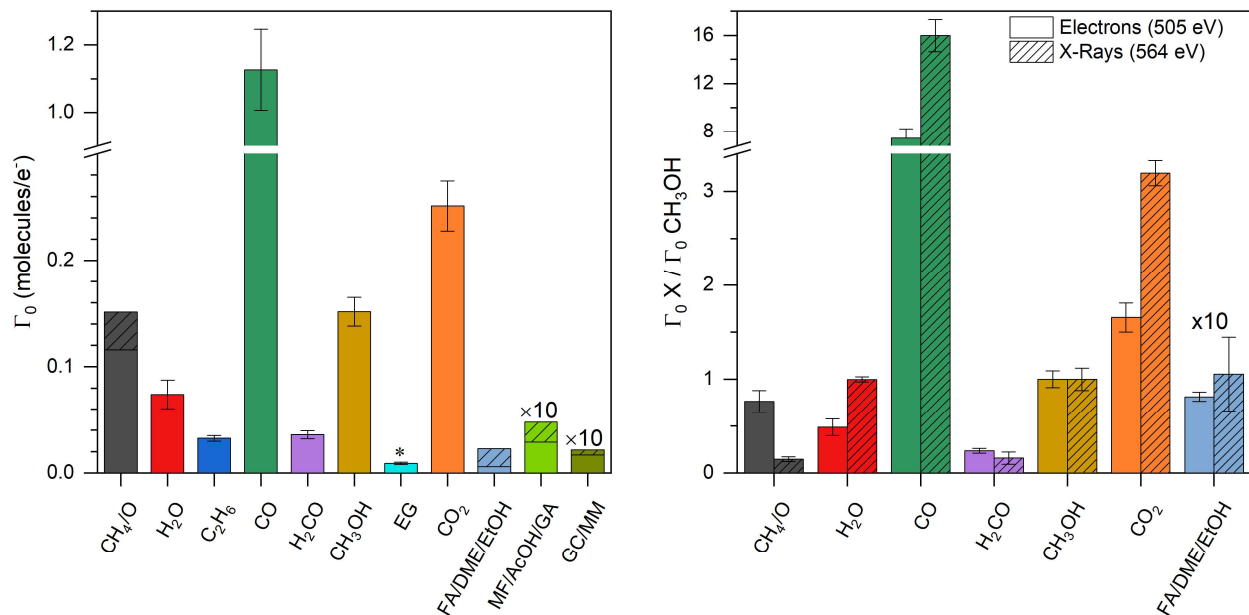


**Figure 3.** (Left) Desorption yields in molecules per incident electron for methanol and products resulting from methanol irradiation with 505 eV electrons. Striped area shows the value range for the corresponding yield when the  $m/z$  cannot be attributed to a single molecule. Asterisk indicates likely overestimation. (Right) Comparison of relative desorption yields between ESD (present work) and X-Ray photodesorption.<sup>[6]</sup> Each data set is normalised to the CH<sub>3</sub>OH yield. Yields for the black and blue data set shown were calculated using the partial ionisation cross-sections for to CH<sub>4</sub> and formic acid (FA), respectively. Names abbreviations are the same as in Figure 2.

### Comparison with X-Ray Photodesorption

In order to discuss the weight of electron induced desorption in the X-ray induced processes, we will now compare the ESD desorption yields obtained here with X-rays desorption yields. First, we discuss the absolute yields, then the kinetics of the process described by the effective depletion cross-section and finally we compare the products seen desorbing in each case.

In the case of 525 - 570 eV X-Rays, most of the photon's energy is expected to be deposited in the KLL Auger electron originating from an O 1s core absorption.<sup>[8]</sup> Said Auger electron has an energy of ~505 eV for condensed methanol,<sup>[13]</sup> and is generated with a 99.4% yield after the photon absorption.<sup>[14]</sup> Therefore, since one absorbed photon results in one Auger electron in the photon irradiation experiments, we compare the X-Ray photodesorption yields in molecules *per absorbed photon* in the desorption relevant depth ( $\Lambda_{\text{des,XRs}}$ ) from Basalgète *et al.*<sup>[8]</sup> directly with the measured yields in molecules *per incident electron*.

The absolute yields are  $0.036 \pm 0.004$ ,  $0.15 \pm 0.01$  and  $0.01$  desorbed molecules per incident 505 eV electron for H<sub>2</sub>CO, CH<sub>3</sub>OH and molecules related to fragment  $m/z$  46, respectively. While the corresponding 564 eV X-Ray (ionisation continuum) yields are  $0.08 \pm 0.03$ ,  $0.49 \pm 0.06$  and  $0.05 \pm 0.02$  molecules per absorbed photon.<sup>[6]</sup> The methanol desorption yield derived from the present experiments agrees well with X-Ray irradiation data, within a factor ~3. This is an exceptional match, considering the uncertainties involved in such experiments. Auger electrons are created in the whole irradiated volume upon X-Ray irradiation, and the thickness involved in desorption has been estimated to be 30 ML which is related to the radius of the secondary electron cloud.<sup>[8]</sup> On the other hand, from the  $\sigma_{\text{eff}}$  value for methanol we estimate the thickness involved in desorption to be around 8 ML

(comparable to the penetration depth of the incoming 505 eV electrons estimated from the electron IMFP) in our experiments, and is related to the dominant energy and/or particle transport mechanism(s) leading to desorption.<sup>[11d]</sup> The factor we find between ESD and X-Ray desorption yields could be explained by the difference in ice thicknesses involved in the desorption processes.

Regarding the kinetics of ESD, as mentioned earlier we obtained an effective methanol depletion cross-section between  $5 \times 10^{-16}$  and  $15 \times 10^{-16}$  cm<sup>2</sup>, with a weighted average of  $(7.7 \pm 0.3) \times 10^{-16}$  cm<sup>2</sup>. For X-Ray photodesorption we have taken the data published by Chen *et al.*<sup>[33]</sup> who irradiated pure methanol ices with 550 eV X-Rays and monitored the composition of the ice with infrared spectroscopy. From their CH<sub>3</sub>OH destruction dynamics with respect to fluence, we estimate a destruction rate on the order of  $10^{-15}$  cm<sup>2</sup>, considering the absorbed photon flux and applying the same fitting procedure as for the ESD data. These values demonstrate that complex chemistry is induced within the film at comparable global efficiency.

The yields relative to methanol ( $\Gamma_0 X / \Gamma_0 \text{CH}_3\text{OH}$ ) for selected products derived from the present work are compared to the ones from X-Ray photodesorption experiments<sup>[6]</sup> in Figure 3, right panel. In general, the chemistry is replicated as exemplified by the good match of relative yields of H<sub>2</sub>CO and  $m/z$  46 contributors (CH<sub>3</sub>OCH<sub>3</sub>, CH<sub>3</sub>CH<sub>2</sub>OH, and HCOOH). For the other products, the yield found during electron irradiation differs more but is still in the same order of magnitude, and notably the ratio H<sub>2</sub>O:CO:CO<sub>2</sub> is the same for electrons and X-rays. Therefore, we attribute the absolute differences to the difficulty in constraining

## RESEARCH ARTICLE

residual gas contributions to the respective mass channels ( $m/z$  16, 18, 28 and 44).

There is, however, one major difference between our results and X-Ray irradiation:  $O_2$  formation and desorption. During X-Ray irradiation, only between 75% and 30% of the  $m/z$  32 signal was attributed to methanol desorption, therefore  $m/z$  31 was taken to quantify the methanol yield.<sup>[8]</sup> Here we observe the opposite,  $m/z$  31 is always in excess with respect to  $m/z$  32, meaning  $m/z$  32 is mostly methanol. One possible explanation for this is that in our experiments  $HO_2$  ( $m/z$  33) is not accumulated in the ice, and therefore is not available for  $O_2$  formation. It has been reported for amorphous water ice electron irradiation that the  $O_2$  yield is dependent on dose-accumulation of precursors.<sup>[38]</sup> Also,  $O_2$  production in water ices irradiated with 100 eV electrons was suppressed when the ice was covered by methanol layers,<sup>[22]</sup> so our observation is consistent with findings in other electron irradiation experiments in the literature. This discrepancy could be related to the different penetration depths and ice thicknesses involved in desorption between electrons and X-Rays, as already discussed, or even to temperature differences (23 K for electron irradiation and 15 K for X-ray irradiation).

The obtained ESD yields and effective depletion cross-section prove, quantitatively, that the desorption mechanism initiated by X-Ray absorption in pure methanol ices is mainly due to the thermalization of the Auger electrons (XESD). Our study also highlights the importance of electron-based experiments performed on astrochemical ice analogues in this energy range ( $10^2$  eV). It is thus a first step toward more systematic studies of binary or tertiary frozen mixtures, the compositions of which mimic interstellar ices, with the aim to unveil the several steps in the high-energy photon-induced non-thermal desorption mechanisms.

## Conclusions

By combining ESD and TPD analyses, we achieved and validated a quantitative description of non-thermal desorption processes from methanol ices irradiated with O (KLL) Auger-like electrons. Absolute desorption yields in molecules per electron and an effective cross-section indicate the efficient desorption of methanol and its depletion in the ice. The rich induced chemistry leads to the desorption of multiple products, such as CO,  $CO_2$ ,  $CH_4/O$ ,  $H_2O$ ,  $H_2CO$ ,  $C_2H_6$  and those related to  $m/z$  46 ( $CH_3OCH_3$ ,  $CH_3CH_2OH$ , and/or  $HCOOH$ ). We report for the first time the desorption of heavy products during electron irradiation, like  $CH_3OCH_2OH$ .

The remarkable matching between electron and X-Ray desorption yields and depletion cross-section for methanol confirms that the desorption mechanism initiated by X-Ray absorption in pure methanol ices is driven by the thermalization of the Auger electrons (XESD).

## Experimental Section

The ultra-high vacuum (UHV) setup is located at the Institut des Sciences Moléculaires d'Orsay (ISMO). It is equipped with a sample holder connected to a closed-cycle helium cryostat, a QMS with an electron ionization source (70 eV) for neutral detection (HAL 301/3F, HIDEN Analytical) and an electron gun (Kimball Physics EGPS-1022E).<sup>[18b]</sup> The methanol ices were

prepared by vapour deposition onto a cold substrate (gold, 23 K) using a doser. To calibrate the ice thickness, the monolayer desorption was identified using TPD experiments with increasing doses.<sup>[39]</sup> The ices were irradiated with  $505 \pm 1$  eV electrons, while recording selected mass channels with the QMS. A bias potential of 25 V was applied to the substrate to retain the secondary low energy electrons created in the ice.<sup>[40,11c]</sup> On/off irradiation steps provide clear signals for correction of background contributions. The electron flux was varied in the  $0.8 \times 10^{13}$  to  $7.1 \times 10^{13}$   $s^{-1} cm^{-2}$  range. The beam spot size was set to  $0.39 \pm 0.03$   $cm^2$ . By assuming pseudo-first order kinetics, a linear fit of the natural logarithm of the desorption signal with respect to fluence is done to obtain desorption yields for a fresh ice ( $Y_0$ ), and the effective cross-section  $\sigma_{eff}$  for the observed signal decay. Data points were fitted up to fluences of  $1 \times 10^{15}$  to  $3 \times 10^{15}$  electrons/ $cm^2$ . The desorption yields  $Y_0$  (counts/e<sup>-</sup>) were converted into absolute desorption values  $\Gamma_0$  (molecules/e<sup>-</sup>) according to a method described previously<sup>[8,11a,11b]</sup> and detailed in the Supporting Information. In summary, it relies on a factor  $k_x$ , obtained by taking into account: i) the calibration of the QMS signal (using the monolayer desorption signal), ii) the electron ionisation cross-sections at 70 eV and iii) the apparatus function (AF) of the QMS. Taking into account the uncertainties of these three parameters, we estimate the uncertainty of the method to be  $\pm 50\%$ .

## Supporting Information Summary

Detailed experimental and data analysis methods are available in the Supporting Information, including references for the electron-ionisation cross-sections used to calculate  $\Gamma_0$ .<sup>[41-51]</sup>

## Acknowledgements

The authors thank Rémi Dupuy for the interesting discussions. This work was supported by the ANR PIXyES project, grant ANR-20-CE30-0018 of the French Agence Nationale de la Recherche, and by the Region Ile-de-France DIM-ACAV+ program. D.T.-D thanks the Erasmus+ Erasmus Mundus programme support.

**Keywords:** astrochemistry • desorption • surface chemistry • mass spectrometry • electron-induced chemistry

- [1] C. Walsh, R. A. Loomis, K. I. Öberg, M. Kama, M. L. R. van 't Hoff, T. J. Millar, Y. Aikawa, E. Herbst, S. L. Widicus Weaver, H. Nomura, *Astrophys. J.* **2016**, *823*, L10.
- [2] E. L. Gibb, D. C. B. Whittet, A. C. A. Boogert, A. G. G. M. Tielens, *Astrophys. J. Suppl. Ser.* **2004**, *151*, 35–73.
- [3] N. Watanabe, A. Kouchi, *Astrophys. J.* **2002**, *571*, L173–L176.
- [4] H. Hidaka, N. Watanabe, T. Shiraki, A. Nagaoka, A. Kouchi, *Astrophys. J.* **2004**, *614*, 1124–1131.
- [5] E. Dartois, M. Chabot, A. Bacmann, P. Boduch, A. Domaracka, H. Rothard, *Astron. Astrophys.* **2020**, *634*, A103.
- [6] M. Bertin, C. Romanzin, M. Doronin, L. Philippe, P. Jeseck, N. Ligterink, H. Linnartz, X. Michaut, J.-H. Fillion, *Astrophys. J.* **2016**, *817*, L12.
- [7] K. I. Öberg, R. T. Garrod, E. F. van Dishoeck, H. Linnartz, *Astron. Astrophys.* **2009**, *504*, 891–913.
- [8] R. Basalgète, R. Dupuy, G. Féraud, C. Romanzin, L. Philippe, X. Michaut, J. Michoud, L. Amiaud, A. Lafosse, J.-H. Fillion, M. Bertin, *Astron. Astrophys.* **2021**, *647*, A35.
- [9] G. A. Cruz-Díaz, R. Martín-Doménech, G. M. Muñoz Caro, Y.-J. Chen, *Astron. Astrophys.* **2016**, *592*, A68.
- [10] R. T. Garrod, V. Wakelam, E. Herbst, *Astron. Astrophys.* **2007**, *467*, 1103–1115.
- [11] a) R. Dupuy, M. Bertin, G. Féraud, M. Hassenfratz, X. Michaut, T. Putaud, L. Philippe, P. Jeseck, M. Angelucci, R. Cimino, V. Baglin, C. Romanzin, J.-H. Fillion, *Nat. Astron.* **2018**, *2*, 796–801; b) R. Dupuy, G. Féraud, M. Bertin, C. Romanzin, L. Philippe, T. Putaud, X. Michaut, R. Cimino, V. Baglin, J.-H. Fillion, *J. Chem. Phys.* **2020**, *152*, 054711; c) R. Dupuy, M. Haubner, B. Henrist, J.-H. Fillion, V. Baglin, *J. Appl. Phys.* **2020**, *128*, 175304.

## RESEARCH ARTICLE

- [12] A. Ciaravella, G. M. Muñoz Caro, A. Jiménez-Escobar, C. Cecchi-Pestellini, L.-C. Hsiao, C.-H. Huang, Y.-J. Chen, *Proc. Natl. Acad. Sci.* **2020**, *117*, 16149–16153.
- [13] J. C. Fuggle, E. Umbach, R. Kakoschke, D. Menzel, *J. Electron Spectrosc. Relat. Phenom.* **1982**, *26*, 111–132.
- [14] M. O. Krause, *J. Phys. Chem. Ref. Data* **1979**, *8*, 307–327.
- [15] N. Timneanu, C. Coleman, J. Hajdu, D. van der Spoel, *Chem. Phys.* **2004**, *299*, 277–283.
- [16] M. Bazin, S. Ptasinska, A. D. Bass, L. Sanche, E. Bureau, P. Swiderek, *J. Phys. Condens. Matter* **2010**, *22*, 084003.
- [17] E. Böhler, J. Warneke, P. Swiderek, *Chem. Soc. Rev.* **2013**, *42*, 9219.
- [18] a) L. A. Sala, Low-Energy Electron Induced Chemistry in Supported Molecular Films, Université Paris-Saclay, **2018**; b) L. A. Sala, I. B. Szymańska, C. Dablemont, A. Lafosse, L. Amiaud, *Beilstein J. Nanotechnol.* **2018**, *9*, 57–65.
- [19] A. Lafosse, M. Bertin, R. Azria, *Prog. Surf. Sci.* **2009**, *84*, 177–198.
- [20] T. D. Harris, D. H. Lee, M. Q. Blumberg, C. R. Arumainayagam, *J. Phys. Chem.* **1995**, *99*, 9530–9535.
- [21] F. Schmidt, P. Swiderek, J. H. Bredehöft, *ACS Earth Space Chem.* **2021**, *5*, 391–408.
- [22] M. C. Akin, N. G. Petrik, G. A. Kimmel, *J. Chem. Phys.* **2009**, *130*, 104710.
- [23] S. Maity, R. I. Kaiser, B. M. Jones, *Phys. Chem. Chem. Phys.* **2015**, *17*, 3081–3114.
- [24] R. I. Kaiser, S. Maity, B. M. Jones, *Angew. Chem. Int. Ed.* **2015**, *54*, 195–200.
- [25] A. Mahjoub, M. J. Poston, K. P. Hand, M. E. Brown, R. Hodyss, J. Blackberg, J. M. Eiler, R. W. Carlson, B. L. Ehlmann, M. Choukroun, *Astrophys. J.* **2016**, *820*, 141.
- [26] M. D. Boamah, K. K. Sullivan, K. E. Shulenberger, C. M. Soe, L. M. Jacob, F. C. Yhee, K. E. Atkinson, M. C. Boyer, D. R. Haines, C. R. Arumainayagam, *Faraday Discuss* **2014**, *168*, 249–266.
- [27] A. G. M. Abdulgalil, A. Rosu-Finsen, D. Marchione, J. D. Thrower, M. P. Collings, M. R. S. McCoustra, *ACS Earth Space Chem.* **2017**, *1*, 209–215.
- [28] N. Sinha, B. Antony, *J. Phys. Chem. B* **2021**, *125*, 5479–5488.
- [29] R. Luna, G. Molpeceres, J. Ortigoso, M. A. Satorre, M. Domingo, B. Maté, *Astron. Astrophys.* **2018**, *617*, A116.
- [30] S. Tanuma, C. J. Powell, D. R. Penn, *Surf. Interface Anal.* **1994**, *21*, 165–176.
- [31] R. Garcia-Molina, I. Abril, I. Kyriakou, D. Emfietzoglou, *Surf. Interface Anal.* **2017**, *49*, 11–17.
- [32] D. Marchione, M. R. S. McCoustra, *Phys. Chem. Chem. Phys.* **2016**, *18*, 29747–29755.
- [33] Y.-J. Chen, A. Ciaravella, G. M. Muñoz Caro, C. Cecchi-Pestellini, A. Jiménez-Escobar, K.-J. Juang, T.-S. Yih, *Astrophys. J.* **2013**, *778*, 162.
- [34] C. J. Bennett, S. Chen, B. Sun, A. H. H. Chang, R. I. Kaiser, *Astrophys. J.* **2007**, *660*, 1588–1608.
- [35] H. Schneider, A. Caldwell-Overdier, S. Coppieters 't Wallant, L. Dau, J. Huang, I. Nwolah, M. Kasule, C. Buffo, E. Mullikin, L. Widdup, A. Hay, S. T. Bao, J. Perea, M. Thompson, R. Tano-Menka, M. Van Tuyl, A. Wang, S. Bussey, N. Sachdev, C. Zhang, M. C. Boyer, C. R. Arumainayagam, *Mon. Not. R. Astron. Soc. Lett.* **2019**, *485*, L19–L23.
- [36] P. Linstrom, **1997**, DOI 10.18434/T4D303.
- [37] T. Hama, M. Yokoyama, A. Yabushita, M. Kawasaki, P. Wickramasinghe, W. Guo, H.-P. Loock, M. N. R. Ashfold, C. M. Western, *J. Chem. Phys.* **2009**, *131*, 224512.
- [38] N. G. Petrik, A. G. Kavetsky, G. A. Kimmel, *J. Chem. Phys.* **2006**, *125*, 124702.
- [39] M. Doronin, M. Bertin, X. Michaut, L. Philippe, J.-H. Fillion, *J. Chem. Phys.* **2015**, *143*, 084703.
- [40] K. Landheer, S. G. Rosenberg, L. Bernau, P. Swiderek, I. Utke, C. W. Hagen, D. H. Fairbrother, *J. Phys. Chem. C* **2011**, *115*, 17452–17463.
- [41] J. D. Wnuk, S. G. Rosenberg, J. M. Gorham, W. F. van Dorp, C. W. Hagen, D. H. Fairbrother, *Surf. Sci.* **2011**, *605*, 257–266.
- [42] H. C. Straub, D. Lin, B. G. Lindsay, K. A. Smith, R. F. Stebbings, *J. Chem. Phys.* **1997**, *106*, 4430–4435.
- [43] R. R. Laher, F. R. Gilmore, *J. Phys. Chem. Ref. Data* **1990**, *19*, 277–305.
- [44] O. J. Orient, S. K. Strivastava, *J. Phys. B At. Mol. Phys.* **1987**, *20*, 3923–3936.
- [45] C. Tian, C. R. Vidal, *J. Chem. Phys.* **1998**, *109*, 1704–1712.
- [46] J. R. Vacher, F. Jorand, N. Blin-Simiand, S. Pasquiers, *Chem. Phys. Lett.* **2009**, *476*, 178–181.
- [47] K. L. Nixon, W. A. D. Pires, R. F. C. Neves, H. V. Duque, D. B. Jones, M. J. Brunger, M. C. A. Lopes, *Int. J. Mass Spectrom.* **2016**, *404*, 48–59.
- [48] M. Zawadzki, *Eur. Phys. J. D* **2018**, *72*, 12.
- [49] J. Kaur, B. Antony, *Int. J. Mass Spectrom.* **2015**, *386*, 24–31.
- [50] P. Možejko, *Eur. Phys. J. Spec. Top.* **2007**, *144*, 233–237.
- [51] A. Bharadvaja, S. Kaur, K. L. Baluja, *Eur. Phys. J. D* **2019**, *73*, 251.